International Journal of
INTELLIGENT SYSTEMS AND APPLICATIONS IN ENGINEERING
ISSN:2147-6799 www.ijisae.org Original Research Paper

An Efficient Pre-Processing Framework for Segmenting Region of Interest from Knee Osteoarthritis X-Ray Images

Ravindra D. Kale*[1], Sarika Khandelwal [2]

Submitted: 25/12/2023 **Revised**: 04/02/2024 **Accepted**: 12/02/2024

Abstract: Pre-processing is primary and essential element of most of the image processing applications especially in classification and prediction problems. Especially in medical applications where images are prone to different noises and poor contrast, even a good descriptor would make the classifier ambiguous. The article presents an efficient pre-processing approach to eliminate the soft tissues from the hard tissues and provide a distinguishable knee gap to identify the grade of Osteoarthritis. Also, the simple statistical approach provide a generalized solution to extract the region of interest required for Kellgren and Lawrence grade classification of the Kaggle dataset images with 5 levels of grade. The proposed framework has the ability to obtain segmented region of interest with better accuracy required for classification.

Keywords: *Pre-processing, image processing, ambiguous, osteoarthritis, region of interest, Kellgren and Lawrence grade, and Kaggle dataset.*

1. Introduction

Knee Osteoarthritis degrades the articular cartilage and is the most common joint disorder seen in one out of five adults as per the survey conducted. Major pathological symptoms include closer joints, sclerosis and osteophytes formation. Mostly the cause is popularly seen in adults, obsessed peoples and people with sedentary lifestyle. The severity stage yields excruciating pain and complete joint arthoplasty. Therefore, for a painless normal life, proper early diagnosis is necessary for clinical treatment [1][2]. There are several imaging modalities to aid medical experts for diagnosing the severe disease which includes MRI, radiography, ultra-sound techniques, and optical coherence tomography. These are the traditionally preferred gold standard tools for diagnosing knee Osteoarthritis [3][4]. Diagnosing Osteoarthritis through physical examination depends on the expertise of the clinician and the sensitivity and the specificity of the diagnostic tools. However, the fact is, the diagnostic tools have poor sensitivity and the specificity due to increased subjectivity [5].The quality of the knee X-ray or MRI (Magnetic resonance imaging) images degrade due to presence of poor foreground-background contrast, undifferentiated tissues and complexity of human knee structure. Medical experts rely on excellent soft-tissue contrast for better diagnosing the level of Osteoarthritis progression. However, knee images are prone to various artifacts and affected by noise due to acquisition systems installed at the clinical site. The similarity in the contrast between fat around the cartilage tissue, fluid and the cartilage most often possess ambiguity during the delineation process. Due to anatomical complexity of human knees results in delineation on bad contrast which consume time and seem to be laborious [6][7]. Also, the interference of noise and corruption due to unwanted artifacts [8], two important factors related at the priory stage comes into existence. The first step is to clean the knee images by removing the noise and the later step is to improve the contrast while preserving the edge details of the region of interest. The peaks and the valleys formed as a result of low intensity pixels representing mostly the backgrounds, femoral bones and the tibial are to be enhanced properly while maintaining the dynamic range of the pixel intensities over the region of interest.

Conventional enhancement techniques such as histogram equalization is unsuitable and perform badly diverging the dynamic range to affect or distort the image brightness level. On the other hand, it also affects some of the crucial features. Traditional method combine the low and high density probabilities of gray levels to widen the gap between them. This helps to sudden increase in cumulative density but worsen the brightness resulting over-enhancement [9].

The paper contributes in following respect:

1. The proposed pre-processing three stage mechanism eliminate the no-relevant regions from the Kaggle knee images distinguished into five severity grades.

[1] *Ph.D. Scholar, Computer Science & Engineering, G H Raisoni University, Amravati, India*
Email:- ravindra.swati2012@gmail.com
ORCID ID :0009-0005-4603-0090
*(Corresponding Author)
[2] *Associate Professor, Department of Computer Science & Engineering, G H Raisoni College of Engineering, Nagpur, India*
Email:- sarikakhandelwal@gmail.com
ORCID ID : 0000-0003-3336-820X

2. The Region of interest in the images and their masks are obtained in the second stage.

3. The last stage obtains the binary image clearly distinguishing the hard tissues and the gap between the upper and lower bone of the knee.

The article is organized in the following respect: The next part of the paper deals with in-depth literature review, section 3 deals with the description of the materials used along with the proposed framework, experimental analysis is part of section 4, and the last section concludes the article.

2. Related Work

The work in [10] used two step pre-processing for the knee images. The first step involved cropping the image by 60 pixels from top and bottom of the image and then enhancing the image by histogram equalization by adjusting the dynamic range of the pixels. The quality of two OAI (Osteoporosis Initiative) and Rani Channamma University (RCU) dataset was improved using the averaging filter and CLAHE in [11]. The averaging filter selected 16 pixels in each epoch over a target pixel and 15 neighbouring pixels. The mean value of the 15 pixels was used to substitute the target value. The X-ray images were scanned in the aforementioned manner and then the knee joint and bony details visibility was increased using the CLAHE technique. The objective of the method was to adjust the intensity of a target pixel concerning its adjacent neighbourhood [12].

The authors in [13] introduced an automatic cropping module to extract the region of interest for improving the classification accuracy. Priory the images were resized to certain dimension and then cropped by navigating the cropping module by segmentation mask of meniscus, femoral, patellar cartridge and the tibial. The bounding box estimated and then proper offset was added to cover other region of interest such as subchondral bone area. The class imbalance problem was solved by data augmentation by rotating the images randomly in -7 to +7 degrees [14]. The rotation mechanism changed the color saturation, contrast and the illumination level of the images. The unclear images after the transformation process were discarded.

To improve the model generalization ability, the author in [15] inspired by the deep-stacked transformation, combined various modality-specific image preprocessing tasks. The radiographs were subjected to rescaling and flipping in horizontal direction, while the MRI images were enhanced, intensity regulated, noise removed, and histogram equalized. The work in [16] adopted default and augmented pre-processing procedures. The training images were partitioned in 80:20 ratio and were subjected to different preprocessing mechanisms. The higher ratio images were cropped, up-scaled, added with noise, flipped horizontally, and contrast adjusted in a stochastic manner. The remaining 20% images were cropped and added to the training set. In the work suggested in [17] all the Kellgren and Lawrence (KL) [18] images were merged and the right oriented images were changed to left. The authors inverted negative channel images and further corrected the contrast using histogram equalization. All the images were re-scaled to specific dimension. The blur effect was mitigated and the texture quality was improved using Laplace variance approach based on thresholding.

3. Materials and Method

The paper considers knee X-ray images from the high quality Kaggle data store. For effective solutions and better performance evaluation plus comparison, researchers all over the globe prefer mostly publicly available datasets. The dataset is freely available at [19]. The dataset is partitioned into three folders: one for training, one for testing and the last for validation. Each folder consists of 5 subfolders corresponding to five different severity grades of knee arthritis.

The grade corresponding to numeric numbers represents 5 classes and includes: 0 for healthy, 1 for doubtful, 2 for minimal, 3 for moderate Osteoarthritis and 4 representing the severe Osteoarthritis case. More than 8000 X-ray images are available in the dataset which are not suitable in terms of clarity and localization. The objective of the proposed segmentation framework is to clearly discriminate the region of interest (knee joint area) so that the distance between the upper and the lower knee balls can be measured which will certainly discriminate five classes. The major challenge in classifying the grades is the resemblance between grade 0 and grade 1 class, grade 1 and grade 2 class as well grade2 and grade 3 class as seen from the X-ray images available in the dataset (Fig.1). Also, the perceptual quality of the images is poor due to noise and improper illumination which puts and extra overhead on the generalization capability of a good segmentation approach. The unwanted regions needs to be properly excluded without losing the relevant information from the knee images. On the other hand, the dynamic level of the pixel range need adjustment to enhance the contrast of the images for clear visibility of the region of interest. This will aid to uplift the inherent features belonging to the region of interest and help the classifier to discriminate the classes without ambiguity. Some of the sample images from the Kaggle dataset belonging to all the five classes from the training folder are depicted in Fig.1 below.

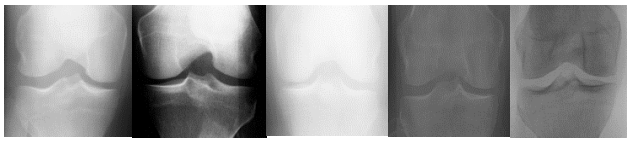

Fig. 1. Knee X-ray images corresponding to Grade 0 (Normal). Samples belonging to good contrast, poor contrast, highly illuminated, poorly illuminated, and negative-like images.

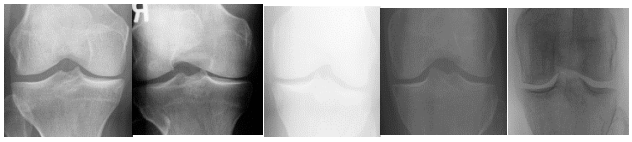

Fig. 2. Similar Knee X-ray images corresponding to Grade 1 (Doubtful).

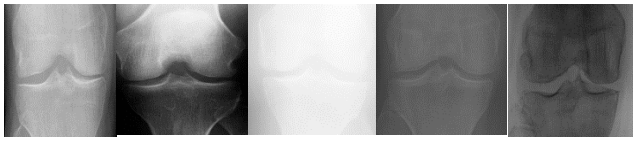

Fig. 3. Similar Knee X-ray images corresponding to Grade 2 (Minimal knee Osteoarthritis).

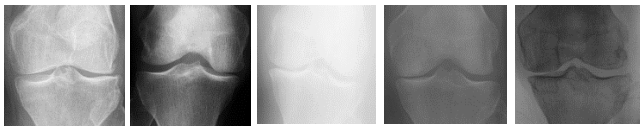

Fig. 4. Similar Knee X-ray images corresponding to Grade 3 (Moderate Class).

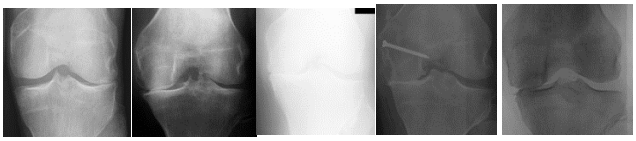

Fig. 5. Similar Knee X-ray images corresponding to Grade 4 (Severe Osteoarthritis Class).

Figures in column 1 (in all Figures from 1 to 5) are clear and can be interpreted clearly for the given grades by a medical expert. Column 2 images have poor contrast and uneven illumination at different regions. The region of interest is affected by poor intensity pixels with respect to other part of the knee regions. It becomes difficult to distinguish grad 1 and grade 2 levels clearly and thus need proper enhancement to extract the region of interest. High illumination is seen in column 3 images which increases ambiguity level and can lead to misclassification as perceived visually. For better analysis, the hard region should be separated from the background so that the grade level can be identified correctly. Very poor illumination is seen in the 4th column images where the background supersede the foreground. The foreground thus must be uplifted so that the background will be distinguished and the gap between the knees joint is visible. The last images show different characteristics with respect to other images. They have negative foreground and background details. Thus developing a common segmentation framework becomes a difficult task to suit and accommodate all the given images under one roof. Either such images need to be eliminated or special arrangements are required which would handle such images and then include such images in the set for pre-processing.

Thus, pre-processing X-ray images becomes a crucial concern before subjecting the images to feature extraction either the traditional way of through blind feature extraction using direct neural network approach. The gap between the knee balls must be known priory for accurate detection of the grades and the neighbouring regions should be clear for better feature extraction to evaluate the heat map caused due to the pressure owing to pain severity in such patients. We present a cropping cum segmentation approach that can successfully eliminate the unwanted region, enhance the region of interest, eliminate noise and binarize the foreground and background for nearly accurate measurement of the distance between the knee joints. Out of 9786 knee X-ray images divided in 5 Kellgren-Lawrence (KL) grades with 224x224 pixel dimension, the percentage of images belonging to each class are shown in Table 1.

Table 1. Percentage of KL-Grade images in the dataset.

KL-Grade	Osteoarthritis Severity	Number of Images (9786)	% of Images
0	Normal or Healthy	3857	40
1	Doubtful	1770	18
2	Minimal	2578	26
3	Moderate	1286	13
4	Severe	295	3

The original image from the grade folder is filtered using the gaussian filter with $\sigma x = 0$ and $\sigma y = 0$ and kernel size of 3x3. The blurring operation is the prerequisite step to eliminate the background from the foreground region. The next step include thresholding the gaussian blurred image using a threshold value = 80. The resultant images obtained after all the three operations is shown in Fig.2. The white region is the foreground and the black region corresponds to the foreground. Further, the binary image is multiplied with the original image to obtain the actual knee region called the mask image which is shown in Fig.3.

Fig. 2. Original Knee image, the gaussian blurred result and the thresholded image.

Fig. 3. The mask image or the knee region of interest.

Experimental analysis showed that the upper and the bottom region of the mask or original image are non-significant as per knee arthritis is considered. To eliminate the non-relevant features from these regions and to reduce the overhead of the classifier, the upper and the bottom area of the knee image were eliminated by cropping the image from both sides. Experimenting over all the images in the dataset, a threshold of 50 rows was considered for elimination from upper and lower part of the image. The cropped image is shown in Fig.4 below. It clearly shows that removing 50 rows from top and the bottom of the image does not affect the region of interest. Fig.4 shows results of various knee images after cropping operation. Here we considered images from all the five grades corresponding to varieties considered in Fig.1.

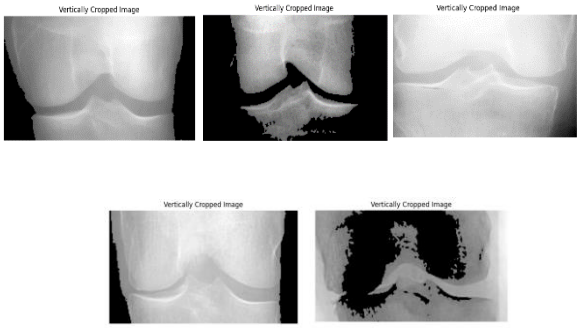

Fig. 4. Result of cropping operation. All the images clearly shows the region of interest. Images are taken from each class sequentially from left to right (Class 0 to class 4).

After vertical cropping, horizontal cropping is carried out to eliminate the unwanted regions from left and right part of the image. The same is done considering each row of the image and finding the occurrence of first extreme non-zero pixels from both ends. The process is completed for all the rows in the cropped image and the most extreme points are considered. Most extreme points are the points which are located in the vicinity of the left and right ends of the image. The results obtained after cropping the image horizontally at the most extreme points is shown in Fig.5. The result after cropping can be seen comparing the first Fig.in Fig.4 and Fig.5. The image was then resized to 128x128 for post operations.

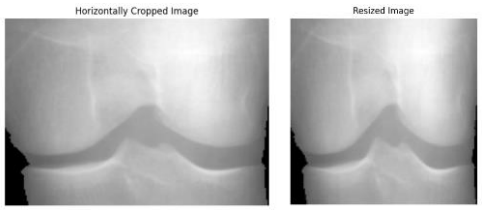

Fig. 5. Image cropped horizontally using the Most extreme points. Resized image (128x128)

We find the strong valley from the points evaluated considering the mean values along each rows. This is done to find the gap region between the knee joints. The pixels intensities at this region differs from the rest of the region. They are darker as compared to hard tissue region. Definitely, the mean along first axis is lower in this region. The circle marked in Fig.6 indicate the gap region which covers a strong valley (Sv). We intended to find the strong valley so as to find the actual region of interest required to improve the classification accuracy. We experimented the technique on several images available in the dataset. Actually, the strong valley point is the function of image contrast. But poor contrast images, uneven illumination, and negative images either shifts the valley point beyond the last peak or decrease the strong nature of the valley thus making it local minima.

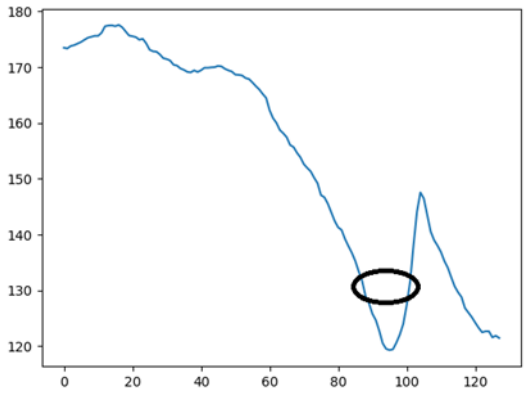

Fig.6. The Strong valley and the gap region marked by the circle.

To compensate, we considered dividing the image into two equal halves I1 and I2 of sizes 128x64 on left and 128x64 on right. Here we found the mean I1m and I2m on both sides along axis=1, the mean along columns of the partitioned images. The global maximum point Sp (strong peak) existing after the strong valley Sv is located in I1m and I2m. The extreme global point Gm is considered by comparing both the global maximum point corresponding to maximum amplitude. For example, if the Strong valley exists at 95, the global maximum is located after 95 up to end. We can see that both the graph of the partitioned images shows global maximum points after the strong valley at 95.

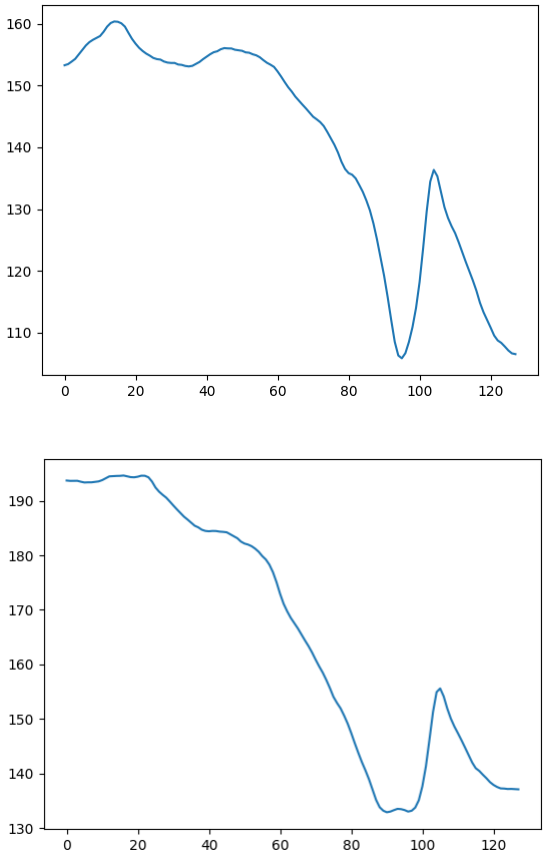

Fig.7. Column Mean values of the partitioned images plotted for finding the maximum points after the valley point in Fig. 6.

If the global maxima in first case occurs at 104 and the second at 105, the peak at 105 is considered. That is, the peak at the extreme end from the right is considered. Without portioning the image may dilute the peak since mean values are considered and the gap portion of the knee is asymmetrical and unbalanced along left and right sides when center of the knee is considered.

Further, we decomposed the mean values of the whole cropped image to three levels using 'db6' mother wavelet and then located the strong valley. The approximation coefficients at level three were considered from start to first global peak and locations of local maxima's were found. The plot representing the approximation coefficients using 'db6' mother wavelet at level three is shown in the Fig.8. Here, the local maxima's at 2, 4, 6 and 9 were located. The index corresponding to the occurrence of first local maxima is considered. Here, in this case, it is at 2. Since, the coefficients are at level three, we multiplied the index by 8 (2x8=16) to compensate the original indexes at which the strong valley was found.

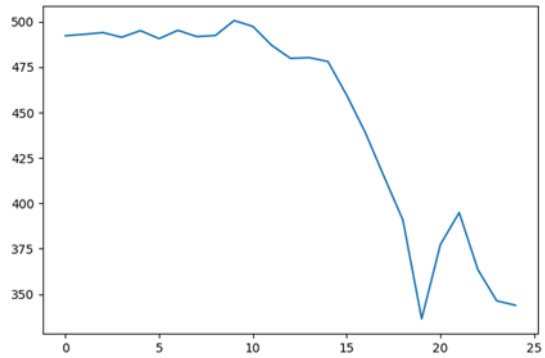

Fig. 8. Wavelet coefficients at level 3 using 'db6' mother wavelet.

Now we have three points, the first local maxima (Lm), the strong valley (Sv) and the extreme global peak (Gp) found using different set of conditions. The final crop points are evaluated using the following conditions:

1. if the index (X-axis coordinate or the row number) of local maxima is greater than the strong valley index and difference of index at strong valley and first local maxima is greater than 50, the image is cropped at:

$$\text{Start\_row} = \frac{L_m + S_v}{2} - 15 \quad (1)$$

$$\text{End\_row} = Gp + 5 \quad (2)$$

The offsets 15 and 5 in both cases are considered to covers the regions in the vicinity instead of cropping the images at the knee gap edges.

2. If the above condition fails under very poor contrast, the image is cropped at the following specific points (row numbers) after experimental evaluations.

$$\text{Start\_row} = 40 \quad (3)$$

$$\text{End\_row} = 110 \quad (4)$$

Note that the row numbers are subjected to the image which had been resized to 128x128 and not the original image. The extracted region of interest is shown in the Fig.9. Finally, the ROI image is median filtered and thresholded using a threshold calculated by estimating the mean of the ROI image. The resultant binarized image is shown in Fig.10 which can be used to estimate the distance between the knee gap and the ROI can be used for conventional or blind feature extraction to improve the classification accuracy of 5 KL grade knee X-ray images.

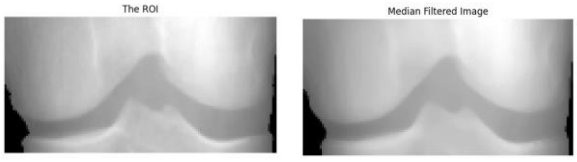

Fig. 9. Extracted region of interest (ROI) after final crop operation. Median filtered image after ROI.

Fig. 10.Binarized image showing clearly the gap between the knees.

The framework for the proposed region of interest extraction is described in Algorithm 1.

Algorithm 1

Input – Original Knee image

Output – Segmented Region of Interest

Read the original image

Blur the image using Gaussian kernel (3x3)

Threshold the blurred image using threshold=80

Multiply the original image and the binary image

Crop the image vertically eliminating 50 rows from top and bottom

Crop the image vertically – Extreme non-zero elements

Resize the image – 128x128

Find Lm, Sv and Gp - the first local maxima, strong valley and extreme global peak

Crop the image using either equation (1) & (2) or (3) and (4)

4. Results and Discussion

Fig.11 shows the original images and the segmented output from each KL-grade classes from top to bottom. The knee gap obtained in the ROI clearly shows the difference and can be used for classification. The first output clearly shows a large gap between the two hard tissues. The distance between the joints in the second output is narrowed in the right lobe. In a similar manner, the spacing reduces for the class 3 and class 4 images. The structure of the inner hard tissues inside the gap and the texture pattern in the neighbourhood of the joint also play an important role in detecting the level of the knee Osteoarthritis. For class 0 (healthy) and 1 (doubtful), significant features pertaining to the lower and upper middle hard tissues need to be extracted. On the other hand, the distance between the upper and lower hard tissue need to be calculated accurately in the minimal osteoarthritis case. Whereas, the area of hard tissues coverage in the gap determines the moderate and the severe osteoarthritis. Considering distance as the primary feature, other textural and structural features can be obtained from the neighbourhood to improve the classification. The accuracy will depend on the quality of other fine and course features which will distinguish the KL-grades properly without ambiguity. We carried experiments over random samples from each class and found the values for thresholding. We experimented with other values of threshold and found that they produces better results of one set of images while their performance degrade on other images. The resultant images shows some distortion with respect to tiny areas which can be eliminated using any threshold based windowing method.

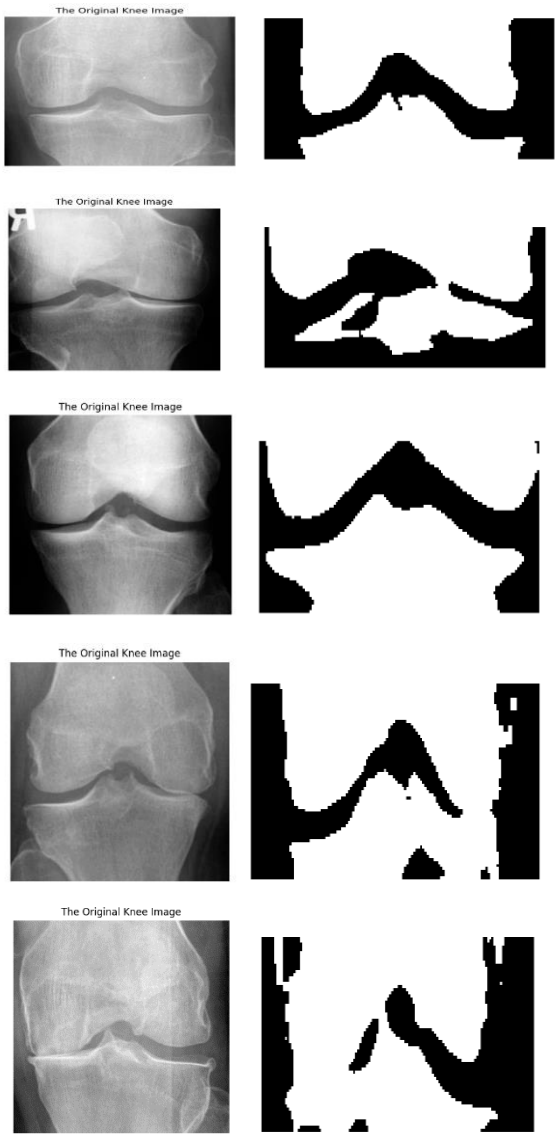

Fig. 11. Original image and their segmented ROI

5. Conclusion

We have not used any contrast enhancement measure to remove the unevenness of the illumination. The segmentation output can be improved by properly controlling the dynamic range of the pixels. The challenge

is to incorporate a generalized system that would fit to all types of images as shown in Fig.1. The images were resized to 128x128, therefore the pixel distance will not measure the accurate distance between the upper and lower hard tissues. This will increase the probability of misclassification between especially class 0, 1 and 2. The proposed framework is able to distinguish the foreground and the background. Also, the unwanted regions are washed out making the ROI better for extracting concentrated and relevant features. The segmented output can be improved by adopting a quality noise removing filter which will retain the edge information and enhance the ROI.

Conflicts of interest

Authors have no conflicts of interest**.**

References

[1] Oka, H., Muraki, S., Akune, T., Mabuchi, A., Suzuki, T., Yoshida, H., Yamamoto, S., Nakamura, K., Yoshimura, N., Kawaguchi, H.: Fully automatic quantification of knee osteoarthritis severity on plain radiographs. Osteoarthritis and Cartilage 16(11), 1300{1306 (2008)

[2] Shamir, L., Ling, S.M., Scott, W., Hochberg, M., Ferrucci, L., Goldberg, I.G.: Early detection of radiographic knee osteoarthritis using computer-aided analysis. Osteoarthritis and Cartilage 17(10), 1307{1312 (2009)

[3] Shamir, L., Ling, S.M., Scott Jr, W.W., Bos, A., Orlov, N., Macura, T.J., Eckley, D.M., Ferrucci, L., Goldberg, I.G.: Knee X-ray image analysis method for automated detection of osteoarthritis. IEEE Transactions on Biomedical Engineering 56(2), 407{415 (2009)

[4] Shamir, L., Orlov, N., Eckley, D.M., Macura, T., Johnston, J., Goldberg, I.G.: Wndchrm{an open source utility for biological image analysis. Source code for biology and medicine 3(1), 13 (2008).

[5] Kellgren, J.H.; Lawrance, J.S. Radiological Assessment of Osteo-Arthrosis. Ann. Rheum. Dis. 1957, 16, 494–502.

[6] Gan, H. S., Tan, T. S., Abdul, K., Ahmad, H., Khairil, A. S., Abdul, K. R., Weng, K. T., Liang, X. W. & Kashif, T. C. 2014. Medical image visual appearance improvement using bihistogrambezier curve contrast enhancement: data from the osteoarthritis initiative. The Scientific World Journal.

[7] Dougherty, Geoff. 2009. Digital Image Processing for Medical Applications. Cambridge University Press.

[8] Dar, S. U., Yurt, M., Karacan, L., Erdem, A., Erdem, E., & Çukur, T. 2019. Image synthesis in multi-contrast MRI with conditional generative adversarial networks. IEEE Transactions on Medical Imaging 38(10): 2375-2388.

[9] Gan, H. S., Tan, T. S, Abdul, K. R., Abdul, K., Ahmad, H., Khairil, A. S., Liang, X. W. & Weng, K. T. 2014. Medical image contrast enhancement using spline concept: data from the osteoarthritis initiative. Journal of Medical Imaging and Health Informatics4: 511-20.

[10] Mohammed, A.S.; Hasanaath, A.A.; Latif, G.; Bashar, A. Knee Osteoarthritis Detection and Severity Classification Using Residual Neural Networks on Preprocessed X-ray Images. Diagnostics 2023, 13, 1380.

[11] Khalid, A.; Senan, E.M.; Al-Wagih, K.; Ali Al-Azzam, M.M.; Alkhraisha, Z.M. Hybrid Techniques of X-ray Analysis to Predict Knee Osteoarthritis Grades Based on Fusion Features of CNN and Handcrafted. Diagnostics 2023, 13, 1609.

[12] Ahmed, S.M.; Mstafa, R.J. Identifying Severity Grading of Knee Osteoarthritis from X-ray Images Using an Efficient Mixture of Deep Learning and Machine Learning Models. Diagnostics 2022, 12, 2939.

[13] Junru Zhong, Yongcheng Yao, Donal Cahill, Fan Xiao, Siyue li, Jack Lee, Kevin Ki-Wai Ho, Michael Tim-Yun Ong, James Griffith and Weitian, "Unsupervised domain adaptation for automated knee osteoarthritis phenotype classification," Quantitative Imaging in Medicine and Surgery, 2023, 13(11), 7444-7458.

[14] Cueva, J.H.; Castillo, D.; Espinós-Morató, H.; Durán, D.; Díaz, P.; Lakshminarayanan, V. Detection and Classification of Knee Osteoarthritis. Diagnostics 2022, 12, 2362.

[15] Md. Rezaul Karim, Jiao Jiao, till Dohmen, Michael Cochez, Oya bayan, Dietrich Rebholz-Schuhmann and Stefen Decker, "DeepKneeExplainer: Explainable Knee Osteoarthritis Diagnosis from Radiographs and Magnetic resonance Imaging," IEEE Access, Vol. 9, 2021, pp. 39757-39780.

[16] Kevin Thomas, Lukasz Kidzinski, Eni Halilaj, Scott Flemming, Guhan Venkatraman, Edwin H. G. Oei, Garry Gold and Scott Delp, "Automated Classification of radiographic knee Osteoarthritis Severity Using Deep Neural Networks," Radiology, Artificial Intelligence, 2020, vol. 2(2):e190065.

[17] Fabi Prezja, Juha Paloneva, Ilkka Polonen, Esko Niinimaki and Sami Ayramo, "Deepfake Knee osteoarthritis X-rays from generative adversial neural

networks deceive medical experts and offer augmentation potential to automatic classification, Scientific Reports, 2022, 12:18573.

[18] Kellgren, J. H. & Lawrence, J. Radiological assessment of osteo-arthrosis. Ann. Rheum. Dis. 16, 494 (1957).

[19] Tiwari, S. Knee Osteoarthritis Dataset with Severity Grading. Kaggle.Availableonline:https://www.kaggle.com/datasets/shashwatwork/knee-osteoarthritis-dataset-with severity?resource=download&select=auto_test